Biometals (2014) 27:731–744
DOI 10.1007/s10534-014-9765-0

Cellular localization and developmental changes of Zip8, Zip14 and transferrin receptor 1 in the inner ear of rats

Dalian Ding · Richard Salvi · Jerome A. Roth

Received: 21 May 2014 / Accepted: 18 June 2014 / Published online: 10 July 2014

Abstract Prior studies have demonstrated that the inner ear can accumulate a variety of essential and potentially toxic heavy metals including manganese, lead, cobalt and cadmium. Metal accumulation is regulated in part by the functionality and affinity of these metals for the different transport systems responsible for uptake across the blood-cochlea barrier and their subsequent uptake into the different cells within the inner ear. Transport of these metals across cell membranes occurs by many of the same transport systems which include DMT1, Zip8 and Zip14. All three metal transporters have been identified in the cochlea based on quantitative PCR analysis. Prior studies in our laboratory examined the localization and developmental changes of DMT1 in rat cochlea and since the two Zip proteins are also likely to contribute to the transport of essential and non-essential divalent cations, we performed immunolabeling experiments in postnatal day three rat pups and adult rats. For comparison, we also immunolabeled the specimens with antibody against transferrin receptor 1 (TfR1) which is important in DMT1-mediated transport of Fe and Mn. Results presented in this paper demonstrate that the cellular and subcellular distribution of both Zip8 and Zip14 within the different components of the inner ear are distinct from that of DMT1. Nuclear localization for both Zip transporters as well as TfR1 was observed. The findings also reveal that the selective distribution of the three proteins was altered during development presumably to meet the changing needs of the cells to maintain normal and functional levels of iron and other essential metals.

Keywords Zip8 · Zip14 · Transferrin receptor · Hair cells · Spiral ganglion neurons · Stria vascularis · Metal transporters

D. Ding
Department of Otolaryngology Head and Neck Surgery, Xiangya Hospital, Central South University, Changsha 410008, Hunan, China
e-mail: dding@acsu.buffalo.edu

R. Salvi
Center for Hearing and Deafness, University at Buffalo, 137 Cary Hall, Buffalo, NY 14214, USA
e-mail: salvi@buffalo.edu

J. A. Roth (✉)
Department of Pharmacology and Toxicology, University at Buffalo, 11 Cary, Hall, Buffalo, NY 14214, USA
e-mail: jaroth@buffalo.edu

Introduction

The inner ear can accumulate a variety of heavy metals including manganese (Mn), lead (Pb), cobalt (Co) and cadmium (Cd). Metal accumulation is regulated, in part, by the functionality and affinity of these metals for the different transport systems which are responsible for uptake across the blood-cochlea barrier and their subsequent transport into different cells within

the inner ear. The unique properties of different metal transporters selectively control uptake of these and other metals into cells within the cochlea thereby influencing normal cellular processes as well as initiating potential neurotoxic responses and the resulting hearing impairment in cases of excess exposures. The combined capacities of these transport systems are ultimately responsible for the net accumulation of these metals within the individual components of the cochlea. For example, Cd, a heavy metal widely used in the production of batteries, solar panels, pigments, and plastic stabilizers has been linked to a wide range of adverse medical conditions including hearing impairment (Basinger et al. 1987; Herber 1992; Bertin and Averbeck 2006; Huff et al. 2007). Similarly, prolonged exposure to Mn, which can induce severe and debilitating dystonic movements resembling Parkinson's disease (Huang et al. 1993; Krieger et al. 1995; Pomier-Layrargues et al. 1995; Olanow et al. 1996; Pal et al. 1999) has also been linked to hearing loss (Khalkova and Kostadinova 1986; Korczynski 2000; Josephs et al. 2005; Park et al. 2006; De Silva and Yamao 2007). Moreover, Co, used in the preparation of magnetic, wear-resistant and high-strength alloys, and Pb, ranked second on the ATSDR/EPA Priority List of Hazardous Substances, have both been reported to cause hearing loss (Pelclova et al. 2012; Liu et al. 2013).

One thing Cd, Mn, Co and Pb have in common is that they are all transported across cell membranes by many of the same transport systems including DMT1, Zip8 and Zip14. DMT1 is generally considered to be the major transmembrane protein responsible for the uptake of these and other potentially toxic divalent metals (Gunshin et al. 1997). In mammals, four isoforms of DMT1 have been identified (Gunshin et al. 1997; Fleming et al. 1998; Hubert and Hentze 2002); the four isoforms differ in their N- and C-terminal sequences with two mRNA isoforms possessing an IRE motif downstream from the stop codon on the message. DMT1-mediated uptake of the transferrin-bound metals, Mn or Fe, is dependent on binding to the transferrin receptor 1 (TfR1) (Roth and Garrick 2003) although transport of these metals via DMT1 can also occur at the cell surface independent of the transferrin pathway. Two members of the solute-carrier-39 (SLC39) zinc metal-transporter family, Zip8 and Zip14, also appear to function in the transport of Fe, Cd, Mn, Co and Pb (He et al. 2006; Liuzzi et al. 2006; Girijashanker et al. 2008; Fujishiro et al. 2011). Unlike DMT1, which is driven by a hydrogen ion gradient, both Zip proteins are divalent cation/HCO^{-3} symporters with the transmembrane HCO^{-3} gradient acting as the driving force for divalent metal transport. There is mounting evidence that both Mn and Cd have relatively high affinity for Zip8 and Zip14 suggesting they may play a more significant role in the transport of these cations although their relative transport efficacy compared to DMT1 is poorly understood. Since the interstitial fluid in brain has a pH of approximately 7.3 (Chesler 2003), which is close to optimal properties for both Zip transporters, their contribution to metal uptake under normal conditions may be greater than that of DMT1, which functions maximally around pH 6.0.

All three metal transporters, DMT1, Zip8 and Zip14, have been identified in the cochlea based on quantitative PCR analysis (Ma et al. 2008). In addition, our recent immunolabeling studies in postnatal day three (P3) and adult rats identified significant developmental changes in the distribution of the different isoforms of DMT1 in rat cochlea (Ding et al. 2014). Since the two Zip proteins are also likely to contribute to the transport of essential and non-essential divalent cations, we performed immunolabeling experiments in postnatal day 3 rat pups and adult rats to determine where Zip8 and Zip14 are located in the cochlea during development versus adulthood. We also immunolabeled the specimens with an antibody against TfR1, which is important in the DMT1-mediated transport of Fe and Mn across the blood–brain barrier and cells within the CNS (Moos 1996; Yang et al. 2011; Gunter et al. 2013).

Experimental procedures

Materials

Rabbit infinity purified polyclonal antibodies were used to identify Zip8 (Sigma SAB3500598), Zip14 (Sigma SAB3500603), and TfR1 (Sigma SAB4501837) in the cochlear tissues. TRITC-conjugated, goat anti-rabbit IgG was used as the secondary antibody against Zip8, Zip14, or TfR1, respectively (Sigma T5268). A mouse monoclonal antibody against neurofilament 200 (Sigma N0142) was used to label spiral ganglion neurons (SGN) and auditory nerve fibers (ANF); Alexa Fluor 488 goat

anti-mouse IgG (Jackson ImmunoResearch Lot# 84763) was used as the secondary antibody. Alexa 488 conjugated phalloidin (Sigma A12379) was used to label F-actin that is heavily expressed in the stereocilia and cuticular plate and circumferential ring of hair cells in adult rats. TO-PRO-3 (Life Technologies T3605) was used to label cell nuclei.

Animals

P3 and adult Sprague–Dawley rats were used for this study (Charles River Laboratories, Wilmington, MA, USA). Animals had free access to water and were fed ad libitum normal rat chow. All experimental procedures were approved by the Institutional Animal Care and Use Committee (IACUC) of University at Buffalo and conform to the guidelines issued by the National Institutes of Health.

Immunocytochemistry

Rats were euthanized with CO_2, decapitated and then the bullae were quickly removed. The apex of the cochlea was opened, the round window membrane punctured and the stapes removed from the oval window. Formalin (10 %) in phosphate buffered saline (PBS) was perfused into the cochlear cavity through either the hole on the apex or the two windows. The bulla was then immersed in above fixative over-night at 4 °C. After rinsing with PBS, the cochlear basilar membrane, spiral ligament containing the stria vascularis and modiolus containing the SGN in Rosenthal's canal were carefully dissected out. The resulting specimens were subsequently incubated with 1 % Triton X 100 and 5 % goat serum in 0.1 M PBS plus primary antibody against Zip8, Zip14 or TfR1 at 4 °C for 24 h. On the second day, specimens were rinsed three times in PBS for 15 min. each and then incubated with TRITC conjugated goat anti-rabbit IgG for 60 min. at room temperature. Afterwards, auditory nerve fibers and SGN in postnatal day three rats were labeled with neurofilament 200 kD mouse antibody overnight at 4 °C in solution containing 20 µl of mouse anti-neurofilament antibody, 20 µl Triton X-100 (10 %), 6 µl normal goat serum, and 154 µl of 0.1 M PBS. Samples were rinsed three times in 0.1 M PBS and immersed in a solution containing 2 µl of Alexa 488 conjugated goat anti-mouse IgG for 60 min as described in our previous publications (Ding et al. 2011a, b, 2012). To identify the stereocilia and cuticular plate of hair cells in adult rats, the organ of Corti was stained with Alexa 488 conjugated phalloidin, which binds to actin, for 30 min. To identify nuclei, specimens were stained with TO-PRO-3 for 20 min. Specimens were mounted on glass slides in glycerin and coverslipped.

Confocal microscopy

Specimens were examined under a confocal microscope (Zeiss LSM-510 Meta) using appropriate filters to detect TRITC-labeled Zip8, Zip14 or TfR1 (excitation 544 nm, emission 572 nm) as described previously (Ding et al. 2011b). The fluorescent signals from Alexa 488 (excitation 495 nm; emission 519 nm) and To-PRO-3 (excitation 642 nm; emission 661 nm) were detected with appropriate filters. Confocal images were processed using Confocal LSM Image Examiner and Adobe Photoshop 5.5 software as described previously (Ding et al. 2011b). Using the Ortho function feature in the Zeiss LSM Image Examiner software, multiple x–y horizontal images were acquired (step size 0.5 µm) to obtain image stacks of the organ of Corti, stria vascularis and SGN. In some cases, horizontal image stacks were merged into a single x–y plane to obtain a surface preparation view of the organ of Corti, stria vascularis or SGN while in other cases images from a single plane were evaluated to determine the location of the protein of interest more precisely. In some cases, Z-plane images were reconstructed from the horizontal image stacks to characterize further the location of a specific protein.

Results

Zip8 and Zip14 in the organ of Corti

Initial studies were performed to compare expression of Zip8 and Zip14 proteins in the organ of Corti of P3 rat pups versus the adult animals. Results of these studies, illustrated in Fig. 1, reveal that Zip8 immunolabeling (red/pink) was expressed in both inner hair cells (IHC) and outer hair cells (OHC) in P3 animals; labeling occurred near or on the surface of the organ of Corti (Fig. 1a, az). In adult rats, Zip8 immunolabeling (red) often overlapped with that of actin (green) resulting in strong yellow labeling throughout the

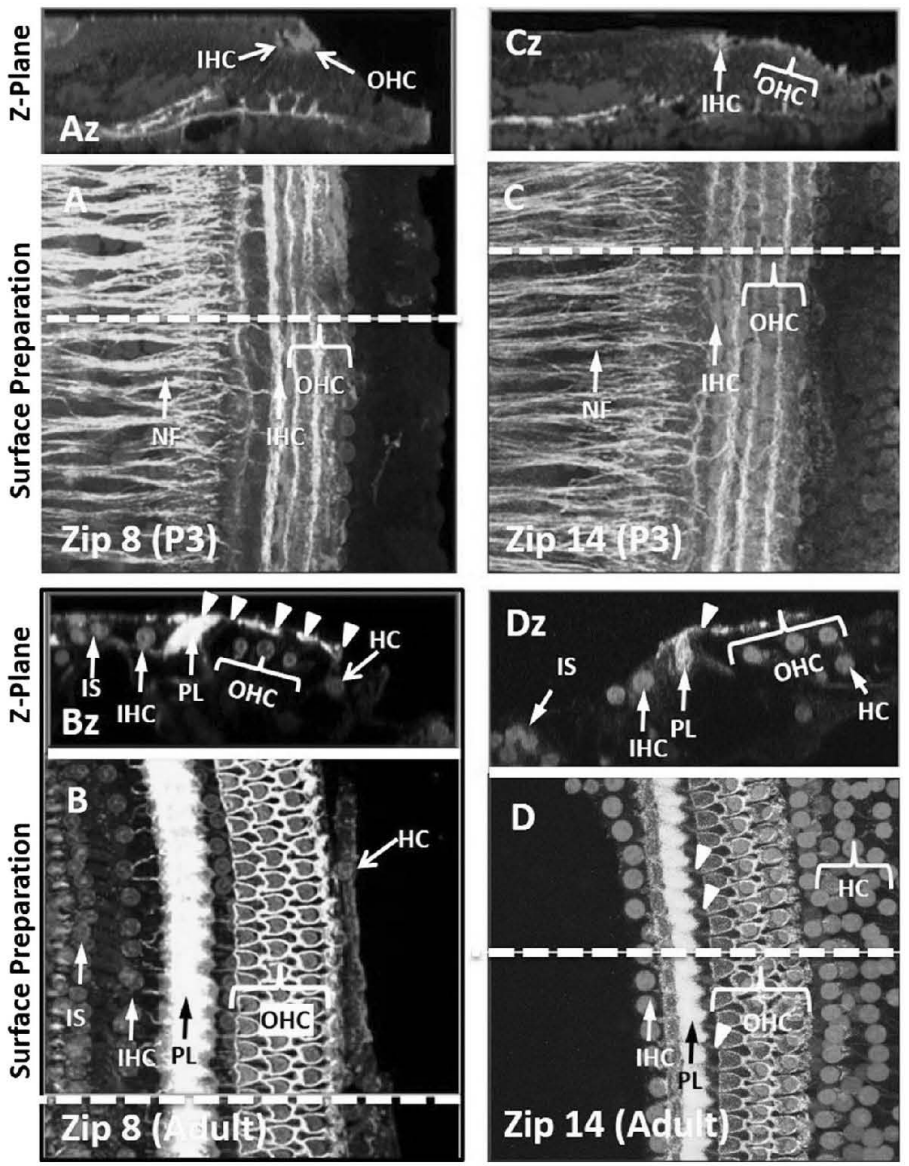

pillar cells (PL) and in the circumferential ring surrounding the OHC near the surface of organ of Corti (Fig. 1bz, arrowheads). Robust labeling was also present in the nuclei of the OHC, IHC, Hensen cells (HC) and support cells in the inner sulcus (Fig. 1b, bz). The location of Zip8 is shown in more detail in surface preparations in which the focal plane was located at the surface of the organ of Corti at the apical pole of the hair cells or at a plane of focus that cut through the nuclei of the hair cells. In P3 rats, Zip8 immunolabeling was present on the apical surface of the organ of Corti (Fig. 2a), but not in the nuclei (Fig. 2b) whereas in adult rats, robust Zip8 immunolabeling was present at the apical surface of the organ of Corti (Fig. 2e) as well as in the nuclei of the hair cells (Fig. 2f).

In P3 rat pups, moderate Zip14 immunolabeling (reddish-orange) was observed mainly on the apical surface of the organ of Corti in the vicinity of OHC and IHC (Fig. 1c, cz); labeling in these regions tended to be somewhat diffuse. In adult rats, strong Zip14 was observed in the nuclei of OHC, IHC, HC and inner sulcus cells (Fig. 1d, dz). In addition, a thin band of Zip14 extended from the pillar cells to the first row of IHC (Fig. 1d, arrowheads). The location of Zip14 is

◀**Fig. 1** Confocal images of Zip8 and Zip14 immunolabeling in surface preparations and Z-plane images of the organ of Corti of P3 rats (*top row*) and adult rats (*bottom row*). **a**, **az** P3 organ of Corti immunolabeled with primary antibody recognizing Zip8 and secondary antibody conjugated to TRITC (*red*); nuclei labeled with TO-PRO-3 (*dark blue*) and nerve fibers (NF) immunolabeled with primary antibody recognizing neurofilament 200 kD and secondary antibody conjugated to Alexa Fluor 488 (*green/turquoise*). *Dashed line* shows the location of Z-plane image in **az**. Zip8 labeling occurred in cytoplasm of IHC and OHC (**az**, **a**; *red/pink*). **b**, **bz** Adult organ of Corti immunolabeled with a primary antibody recognizing Zip8 and secondary antibody conjugated to TRITC (*red*); nuclei labeled with TO-PRO-3 (*dark blue*) and nerve fibers (NF) immunolabeled with primary antibody recognizing neurofilament 200 kD and secondary antibody conjugated to Alexa Fluor 488 (*green/turquoise*). *Dashed horizontal line* in **b** shows location of the Z-plane image in **bz**. Zip8 (*red/yellow*) moderately expressed on the surface of the organ of Corti (*arrow*, **bz**) and heavily expressed in the pillar cells (PL, *yellow*) and nuclei of IHC, OHC, Hensen cells (HC) and inner sulcus cells (*red/pink*). **c**, **cz** P3 organ of Corti immunolabeled with primary antibody against Zip14 conjugated to a secondary antibody labeled with TRITC (*red*); nuclei labeled with TO-PRO-3 (*dark blue*) and nerve fibers (NF) immunolabeled with primary antibody against neurofilament 200 kD and secondary antibody conjugated to Alexa Fluor 488 (*green/turquoise*). *Dashed horizontal line* in **c** shows the location of Z-plane image in **cz**. Moderate to intense Zip14 labeling seen in apical surface of IHC and OHC. **d**, **dz** Adult organ of Corti immunolabeled with primary antibody against Zip14 conjugated to a secondary antibody labeled with TRITC (*red*); nuclei labeled with TO-PRO-3 (*dark blue*) and nerve fibers (NF) immunolabeled with primary antibody recognizing neurofilament 200 kD and secondary antibody conjugated to Alexa Fluor 488 (*green/turquoise*). *Dashed horizontal line* in **d** shows the location of the Z-plane images in **dz**. Moderate to intense Zip14 (*red*) expressed in nuclei of IHC, OHC, Hensen cells (HC) and inner sulcus (IS) cells. Note thin bands of Zip14 extending from pillar cells (PL) and first row of OHC (*red*, *arrowheads*). (Color figure online)

shown in more detail in surface preparations in which the focal plane was located at the surface of the organ of Corti at the apical pole of the hair cells or with the focal plane at the nuclei of the hair cells. In P3 rats, strong Zip14 immunolabeling was present on the apical surface of the organ of Corti (Fig. 3a), but not in the nuclei (Fig. 3b) whereas in adult rats, moderate Zip14 immunolabeling was present at the apical surface of the organ of Corti (Fig. 3a) and also in the nuclei of the hair cells (Fig. 3f).

Zip8 and Zip14 in SGN

In P3 rat pups, little or no Zip8 immunolabeling was detected in SGN or the surrounding supporting cells (Fig. 4a). However, in adult rats, Zip8 immunolabeling was expressed in both the cytoplasm and nucleus of the soma (Fig. 4b, arrows). In P3 rat pups, however, moderate Zip14 immunolabeling was expressed in the nucleus, but not in the cytoplasm of the SGN or in the surrounding supporting cells (Fig. 4c). In adult rats, robust Zip14 immunolabeling was observed in the nuclei of SGN, but not in the surrounding cytoplasm nor in surrounding supporting cells (Fig. 4d, arrow).

Zip8 and Zip14 in stria vascularis

In P3 rat pups, moderate Zip8 expression was located on the apical surface of MC facing the endolymph and in basal cells (BC) deeper in the stria (Fig. 5a, az). Bright Zip8 puncta could often be seen within the hexagonal band of F-actin surrounding the MC profiles (Fig. 5a). When the stria vascularis was fully developed in adult rats, Zip8 was weakly expressed in BC, but largely absent from the green F-actin hexagonal profiles of the MC (Fig. 5b). Within the BC layer, Zip8 labeling was mainly present near the junction of stria vascularis and spiral prominence (Fig. 3b, bz). In P3 rat pups, light Zip14 immunolabeling was seen on apical surface of the spiral prominence (Fig. 5c, cz). In adult rats, however, light to moderate Zip14 staining was observed near the apical surface of MC facing the endolymph and in the deeper BC layer (Fig. 5d, dz). The Zip14 labeling in MC mainly occurred in nuclei (Fig. 5d, pinkish blue) and not in the cytoplasm of the green F-actin hexagonal MC profiles.

TfR1 in organ of Corti, spiral ganglion, stria vascularis

Because TfR1 is important for the uptake of Fe and Mn by DMT1, expression of TfR1 was also examined in the organ of Corti, SGN and stria vascularis. In P3 rat pups, TfR1 immunolabeling was undetectable in the organ of Corti (Fig. 6a, az). In adult rats, however, moderate to intense TfR1 immunolabeling was seen in the nucleus of IHC, OHC, Deiters cells (DC) and HC; the nuclei of support cells in the inner sulcus were lightly stained (Fig. 6b, bz). In SGN, intense TfR1 labeling was observed in the cytoplasm of P3 SGN (Fig. 6c) and in the cytoplasm and nuclei of adult SGN (Fig. 6d). TfR1 was also highly expressed in cytoplasm of MC of stria vascularis in P3 rat (Fig. 6e). In adult rats, however, moderate to intense TfR1 immunolabeling was observed in the nuclei of MC,

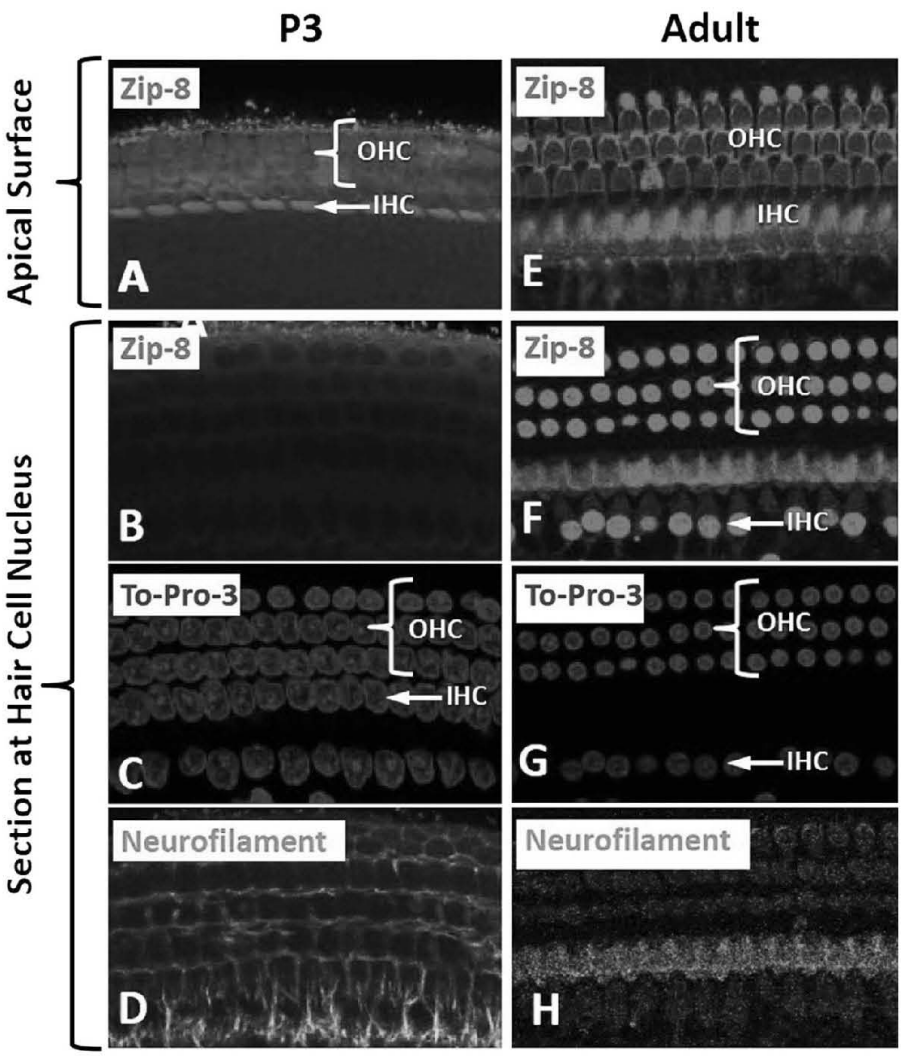

Fig. 2 Confocal images of surface preparations of the organ of Corti; image plane at the apical surface of the hair cells (*top row*) and in the plane of the hair cell nuclei (*lower three row*). Samples immunolabeled for Zip8, TopPro-3 and neurofilament 200 kD. At P3, Zip8 was present on apical surface of IHC and OHC (**a**), but not in the cytoplasm or nucleus (**b**); **c** and **d** show nuclei and nerve fiber in image plane of the hair cell nuclei. In adult rats, Zip8 was present at the apical surface of OHC and IHC (**e**) and in the nuclei of OHC and IHC (**f**); **g** and **h** show nuclei and neurofilament labeling in the image plane of the hair cell nuclei

intermediate cells and BC of the stria vascularis (Fig. 6f, fz). More detailed information on the location of TfR1 immunolabeling was obtained from confocal images obtained in a focal plane located at the surface of the organ of Corti at the apical pole of the hair cells or a focal plane located at the nuclei of the hair cells. In P3 rats, TfR1 was absent from the apical surface of the organ of Corti (Fig. 7a) and nuclei (Fig. 7b). However, in adult rats, moderate TfR1 immunolabeling was present at the apical surface of the organ of Corti (Fig. 7e) mainly in the cuticular plate and stereocilia of the hair cells. In addition, robust TfR1 immunolabeling was present in the nuclei of adult OHC while only mild to moderate labeling was evident in the nuclei of IHC (Fig. 7f).

Discussion

Maintenance of intracellular levels of Fe and other essential heavy metals is regulated by a variety of import and export transporters that adapt to the needs of cells under a variety of conditions (Garrick 2011). Numerous redundant processes are responsible for dynamically controlling homeostatic concentrations of essential metals in order to prevent deficiencies or toxicities. The contribution of each process to the overall accumulation is dependent on the levels of each in any given cell, the relative affinity of the metal for the transporters and the efficiency and capacity for the actual movement of the cation across the cell membrane. Each of these is affected by a variety of factors including pH and the co-

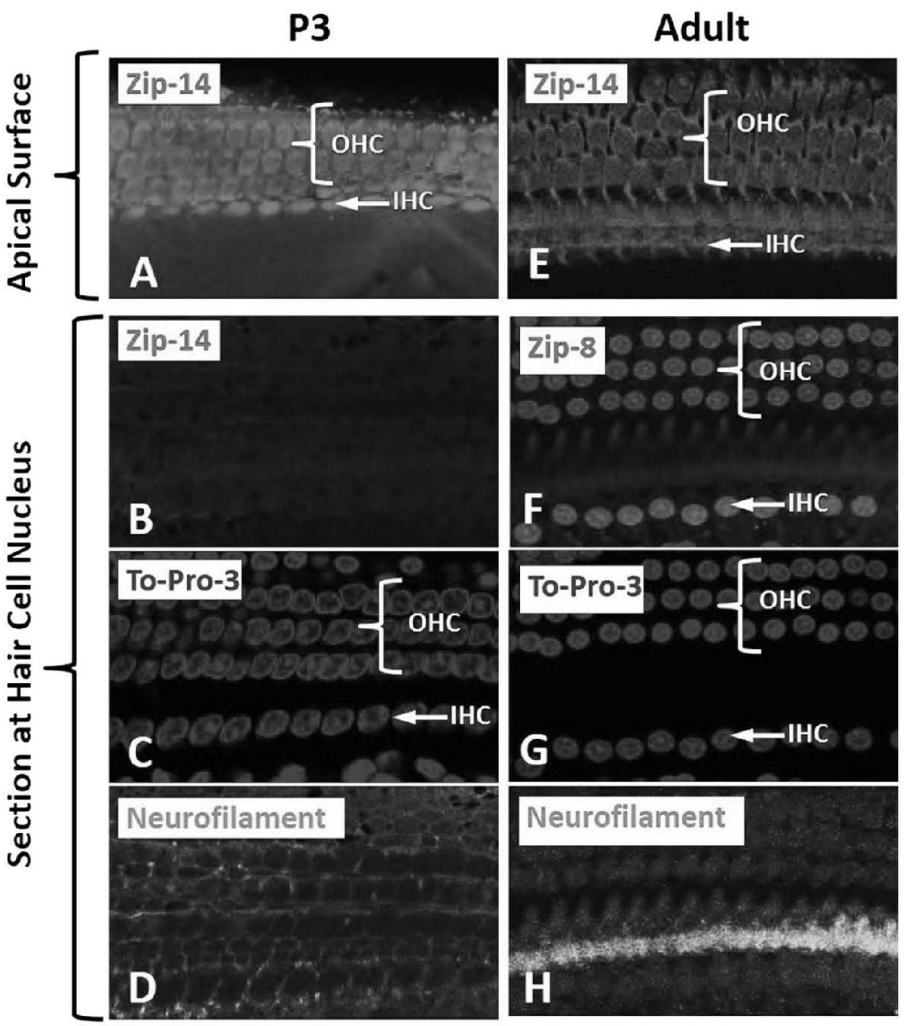

Fig. 3 Confocal images of surface preparations of the organ of Corti; image plane at the apical surface of the hair cells (*top row*) and in the plane of the hair cell nuclei (*lower three row*). Tissues immunolabeled for Zip14, TopPro-3 and neurofilament 200 kD. At P3, Zip14 was present on apical surface of IHC and OHC (**a**), but not in the cytoplasm or nucleus (**b**); **c** and **d** show nuclei and nerve fiber in image plane of the hair cell nuclei. In adult rats, Zip14 was present at the apical surface of OHC and IHC (**e**) and in the nuclei of OHC and IHC (**f**); **g** and **h** show nuclei and neurofilament labeling in the image plane of the hair cell nuclei

transporter ion which may, in part, be the driving force for transport. In the case of divalent metal transport, there are essentially three major carrier mediated systems, DMT1, Zip8 and Zip14. (Garrick et al. 2006; He et al. 2006; Girijashanker et al. 2008). DMT1 is an H^+ dependent process whereas both Zip carriers are HCO_3^- symporters. Quantitative PCR studies using the mRNA extracted from the entire cochlea suggest that DMT1 is the predominant metal transporter and is more abundant than Zip8 and Zip14. This difference, however, does not necessarily imply that DMT1 is the major transporter in all cells in the cochlea as prior studies in our laboratory using P3 and adult rats reveal that all three isoforms of DMT1 are independently expressed in different cell populations (Ding et al. 2014).

For the Zip8 transporter, Cd^{+2} has been reported to display the highest affinity, possessing a Km of 0.62 μM, though Mn^{+2} has been proposed to be the most efficient essential divalent cation transported having a Km for uptake of 2.2 μM (He et al. 2006). Recent studies, however, have questioned this, as the relative uptake of Mn in Zip8 transfected oocytes was considerably lower when compared to that of either Cd or Fe (Wang et al. 2012). Fe loading was also shown to increase both total and cell-surface levels of Zip8 in H4IIE rat hepatoma cells. Among the14-member Zip protein family, Zip14 is most homologous to Zip8 (Girijashanker et al. 2008). Like DMT1, Zip14 has a relatively broad substrate specificity capable of transporting a variety of divalent cations including Zn, Cd, Fe, Mn, Ca, Co, Ni and Pb (Pinilla-Tenas et al. 2011). Two forms of Zip14 have been identified, A and B, having affinities for Mn^{+2} of 4.4 and 18.2 μM respectively (Girijashanker et al. 2008). The highest

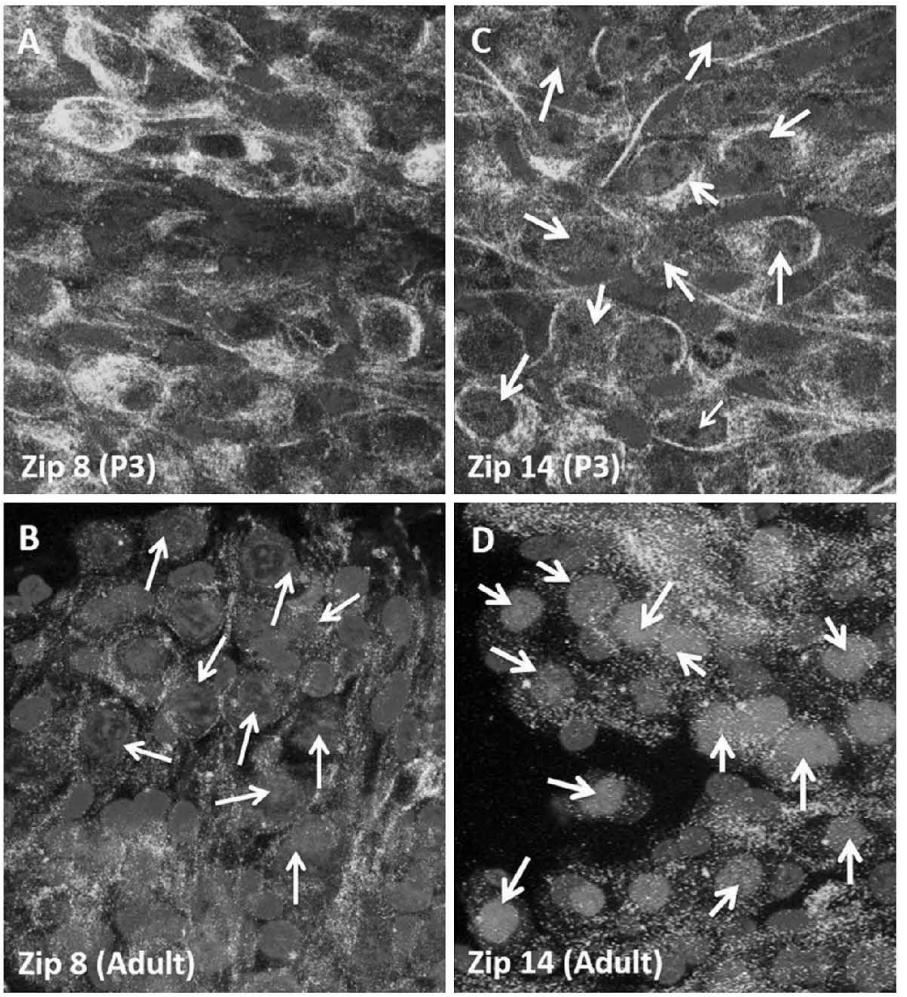

Fig. 4 Confocal images (image thickness 0.5 μm) of spiral ganglion neurons in P3 rats (*top row*) and adult rats (*bottom row*) immunolabeled with Zip8 (*red*) or Zip14 (*red*); nuclei labeled with TO-PRO-3 (*blue*) and nerve fibers (NF) immunolabeled with neurofilament 200 kD (*green*). **a** Zip8 immunolabeling not detected in spiral ganglion neurons in P3 rat. **b** Zip8 expressed in the cytoplasm and nucleus of spiral ganglion neurons in adult rat (*arrows*). **c** Zip14 expressed in nuclei of spiral ganglion neurons in P3 rat (*arrows*). **d** Strong Zip14 labeling in the nuclei of spiral ganglion neurons in adult rat (*arrows*). (Color figure online)

levels of Zip14A are observed in the lung, testis, and kidney whereas the B species of the transporter is relatively evenly distributed. High expression of Zip14 has also been observed in the intestines where it has the potential to play a significant role in the uptake of Fe and Mn although direct quantification relative to that of DMT1 has not been established. Expression of the hemochromatosis protein, HFE, promotes a decrease in both Zip14-dependent transferrin-bound and non- transferrin-bound iron uptake as well as protein levels of Zip14 with no apparent change in the mRNA level suggesting that HFE decreases the stability of Zip14 (Gao et al. 2008).

As noted in the introduction, many of the metals transported by Zip8 and Zip14 have been reported to produce hearing deficits or cochlear damage (Ding et al. 2011b; Liu et al. 2014). The role of these protein in regulating transport and the subsequent accumulation of these ototoxic divalent cations within the inner ear may likely be the rate limiting step controlling their selective deleterious actions. Thus, the distribution of these transporters in the inner ear is important for understanding their contribution in the development of hearing loss.

Zip8 and Zip14 localization in organ of Corti during development

Zip8 and Zip14 metal transporters are restricted to distinct cell types in the cochlea, which like DMT1, changes during development. For example, Zip8 was mainly located in the cytoplasm and on the apical pole of hair cells within the organ of Corti in P3 rats whereas in adults it was mainly located on the apical

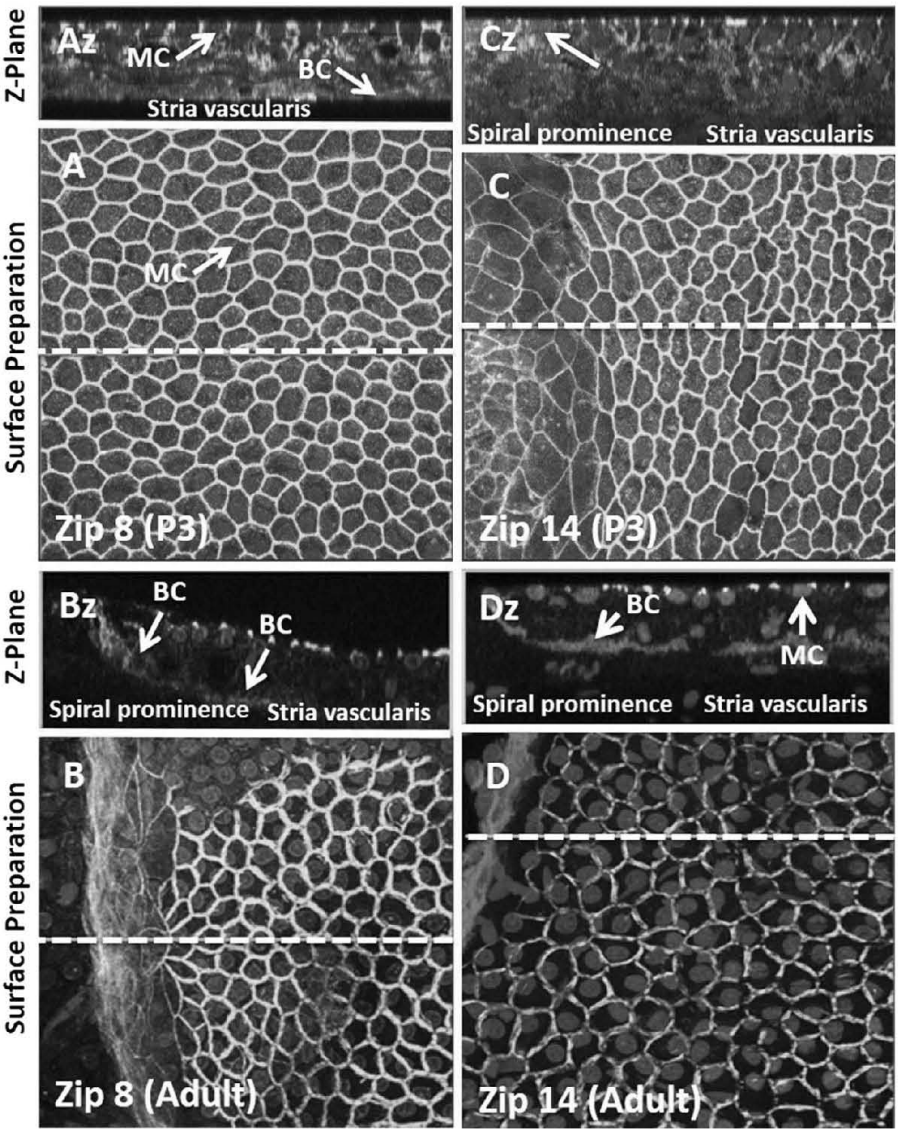

Fig. 5 Confocal images of Zip8 (*left column*) and Zip14 (*right column*) in surface preparation and Z-plane of stria vascularis of P3 rat (*top row*) and adult rat (*bottom row*). **a** Zip8 (*red*) expressed in cytoplasm of marginal cells (MC, *arrow*) and basal cells (BC, *arrow*) of stria vascularis in P3 rat. **b** Zip8 only expressed in BC (*arrow*) in stria vascularis and spiral prominence of adult rat. **c** Zip14 expressed in MC of spiral prominence and stria vascularis in P3 rat. **d** Zip14 intensely expressed in BC of stria vascularis and in nuclei and cytoplasm of epithelium of stria vascularis. Nuclei labeled with TO-PRO-3 (*blue*). F-actin labeled with phalloidin conjugated to Alex Fluor 488 (*green*); note hexagonal ring of F-action surrounding MC. (Color figure online)

surface of hair cells, heavily expressed in in pillar cells and in the nucleus of hair cells, Hensen cells and inner sulcus cells. Zip14 staining patterns in P3 rats was similar to that of Zip8 being primarily located on the apical surface of hair cells. In contrast, in adult rats, Zip14 was not only expressed on the apical surface of hair cells, but was also abundant in the nuclei of IHC, OHC, Hensen cells and inner sulcus cells as well as in a thin strip extending from the pillar cells to the first row of OHC. This is the first report of the Zip proteins being present in the nucleus and parallels the observation of the presence of DMT1 in the nucleus (Roth et al. 2000). As noted in our recent report (Ding et al. 2014), all three forms of DMT1 (1A, -IRE, and +IRE) were undetectable in the organ of Corti of P3 rats using affinity purified antibodies selective for the 1A, -IRE, and +IRE epitopes. Translation of the 1B isoform of DMT1 begins at exon 2 which is common to all four isoforms of the transporter. Thus, the presence of Zip8 and Zip14 in immature animals implies that they are the major transporters for iron and other essential divalent cation (Ding et al. 2014). In adult rats, the 1A, +IRE and −IRE isoforms of DMT1 were mainly detected in thin fibers in the organ of Corti whereas Zip8 and Zip14 were mainly detected in nuclei of hair cells and supporting cells in the organ of Corti. Thus, in the mature organ of Corti, the two Zip proteins appear to be located mainly in the nuclei of different

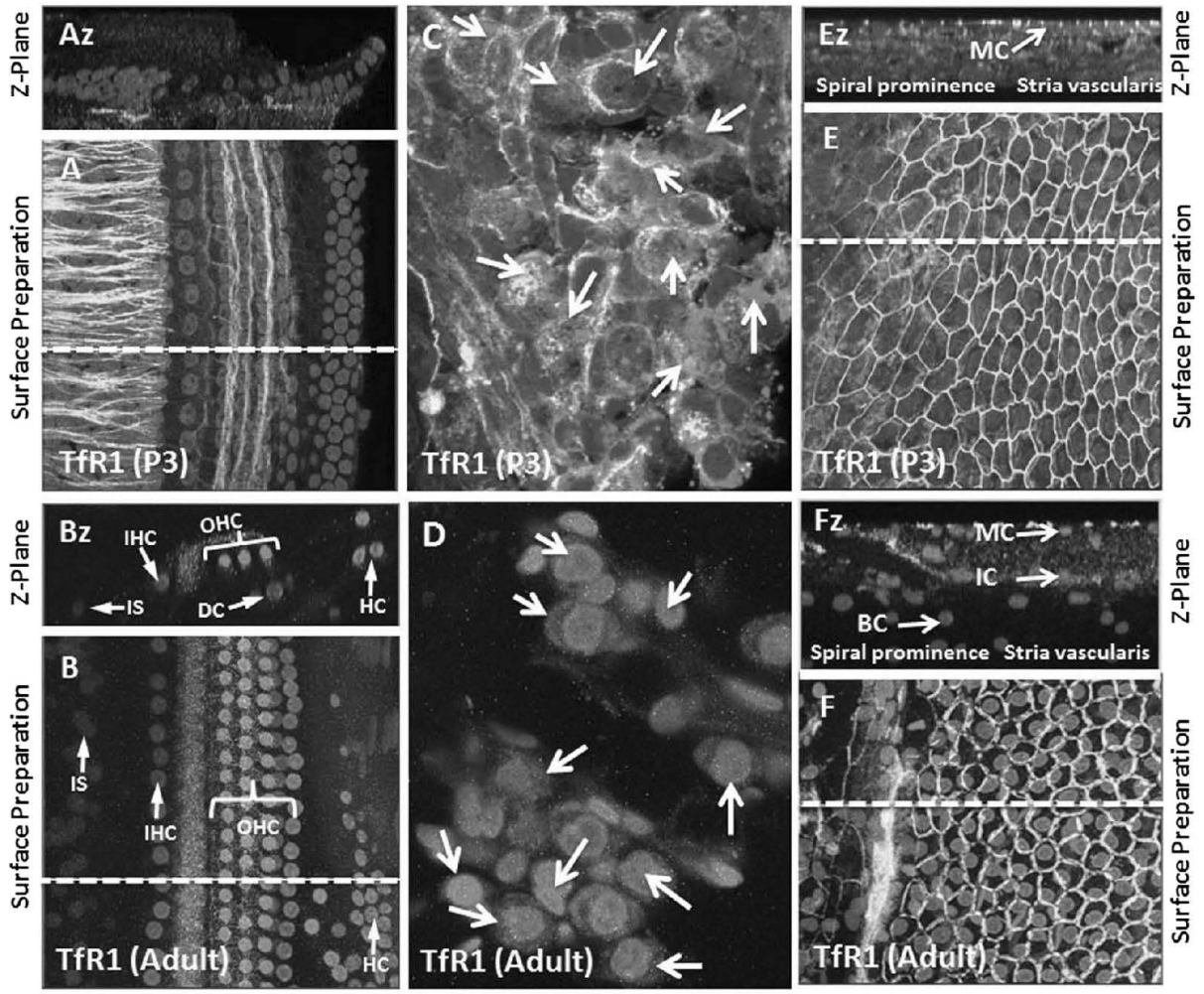

Fig. 6 Confocal images showing TfR1 immunolabeling in surface preparation and Z-plane images of organ of Corti (*left column*), spiral ganglion neurons (*middle column*), and stria vascularis (*right column*). Results shown for P3 rats (*top row*) and adult rats (*bottom row*). Specimens immunolabeled with primary antibody recognizing TfR1 and secondary antibody conjugated to TRITC (*red*); nuclei labeled with TO-PRO-3 (**a**–**f**; *blue*); nerve fibers labeled with antibody against neurofilament 200 kD and Alexa Fluor 488 conjugated secondary antibody (*green/turquoise*) (**a**, **c**); F-actin labeled with phalloidin-conjugated Alexa Fluor 488 (**e**–**f**). **a**, **az** TfR1 not detectable in organ of Corti or auditory nerve fibers (*green/turquoise*) in P3 rat. **b**, **bz** TfR1 intensely expressed in the nuclei of IHC, OHC, HC and lightly expressed in nuclei of the inner sulcus (IC) in adult rat. **c** TfR1 expressed in cytoplasm of spiral ganglion neurons in P3 rat. **d** TfR1 heavily expressed in nuclei and cytoplasm of adult spiral ganglion neurons. **e** TfR1 expressed in cytoplasm of marginal cells (MC) of stria vascularis (*arrow*) in P3 rat. **f** TfR1 immunolabeled nuclei of MC, intermediate cells (IC) and basal cells (BC) in stria vascularis in adult rat. (Color figure online)

cells in the organ of Corti whereas the three DMT1 isoforms are located in nerve fibers suggesting fundamentally different roles for Zip8 and Zip14 compared to DMT1.

Zip8 and Zip14 in SGN during development

Comparison of the two Zip proteins in the SGN during development revealed that Zip14, but not Zip8, was expressed in the nucleus of P3 animal, however, both were heavily expressed in the nuclei of adult SGN. In contrast, the staining pattern for DMT1 in P3 SGN was distinct from Zip8 and Zip14 and greatly dependent on which form of DMT1 was evaluated. For example, the 1A isoform was confined to vesicles within the cytoplasm of SGN, but similar to Zip14, DMT1-IRE immunolabeling was detected within the nucleus and cytoplasm of the P3 SGN. In contrast, the +IRE

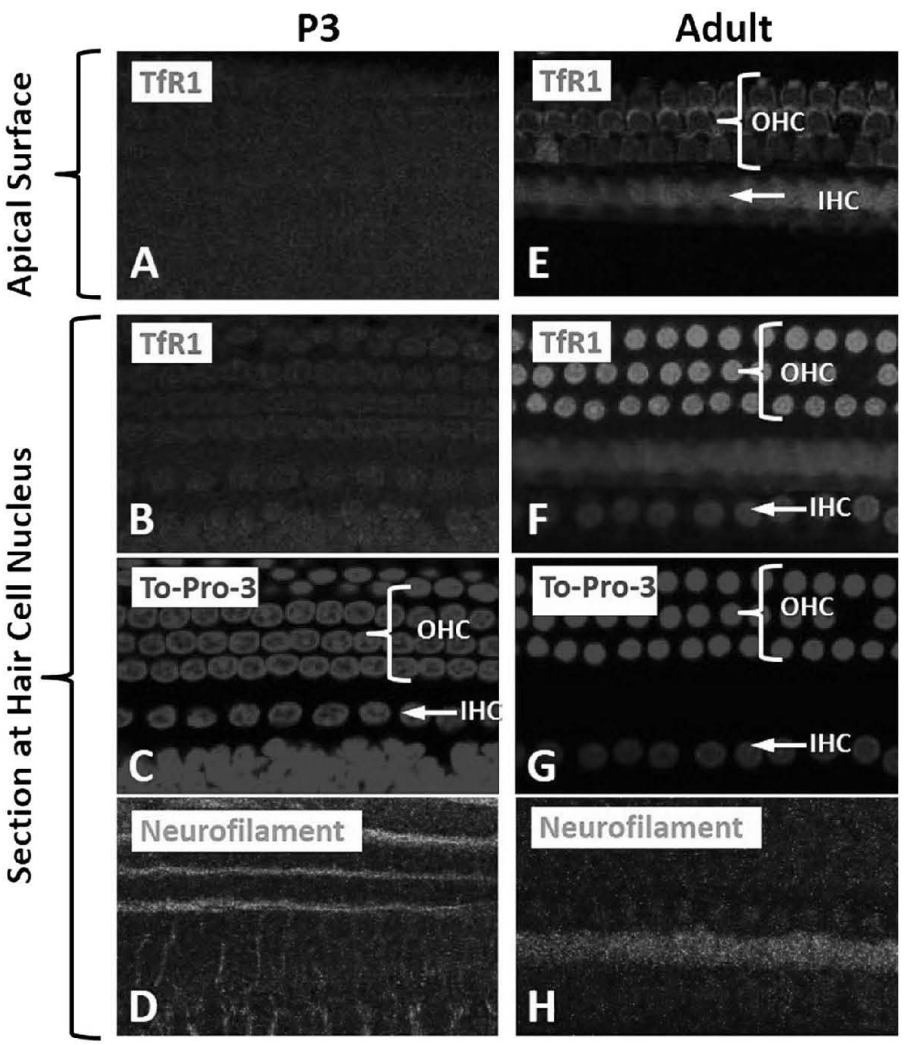

Fig. 7 Confocal images of TfR1, TopPro-3 and neurofilament 200 kD immunolabeling of surface preparations of the organ of Corti; image plane at the apical surface of the hair cells (*top row*) and in the plane of the hair cell nuclei (*lower three row*) (see Fig. 1 for details). At P3, TfR1 was absent from the apical surface of organ of Corti (**a**) and absent from the cytoplasm nucleus of the hair cells (**b**); **c** and **d** show nuclei and nerve fiber in image plane of the hair cell nuclei. In adult rats, TfR1 was present at the circumferential ring of the OHC and at the surface of the IHC (**e**) and in the nuclei of OHC and IHC (**f**); **g** and **h** show nuclei and neurofilament labeling in the image plane of the hair cell nuclei

isoform was only weakly detected in supporting cells surrounding SGN. In adult rats, DMT1 1A labeling was expressed in the cytoplasm of SGN whereas the -IRE species was primarily observed in the cytoplasm of the SGN and occasionally the nucleus and cytoplasm.

Zip8 expression in P3 rats (Fig. 5) was localized on the surface membranes of the stria vascularis as well as MC and BC, similar to the organ of Corti. Labeling of Zip8 in the adult was still relatively strong in BC but its presence in MC was greatly diminished. Staining of Zip14 in P3 rats was observed in the epithelium of spiral prominence but also weakly in MC of stria vascularis. In contrast, Zip14 protein was expressed in BC and MC of stria vascularis in the adult rat as well as the nucleus of the epithelium. In comparison, all three DMT1 isoforms exhibited moderate to strong staining in the stria vascularis of P3 rats and was confined to the outer marginal cell layer that faces the endolymph whereas little or no DMT1 labeling was observed in the intermediate cell and BC layers (Ding et al. 2014). In adult rats, DMT1 1A immunolabeling was observed in the intermediate cell layer of stria vascularis but was also evident in the MC. The -IRE isoform was mainly detected near the surface of MC and also in tubular projections between the marginal cell and intermediate cell layers of the stria vascularis, whereas the +IRE species was expressed near the surface of the MC facing the endolymphatic space. Again, these data illustrate the variations in location of the two Zip transporters in comparison with that of DMT1.

Developmental shift of TfR1expression in cochlea

Expression of TfR1 was also assessed in P3 and adult rat inner ear as its presence is important in the cellular uptake of iron by DMT1. TfR1 has previously been reported to be present in neurons in several brain regions, but conspicuously absent in astrocytes, oligodendrocytes, or microglial cells (Moos 1996) though more recent studies confirmed its presence in oligodendrocytes, the major iron storage cell in brain (Yang et al. 2011). It was also detected in brain and choroid plexus epithelium consistent with its role in the transport of iron across the blood brain barrier. Prior studies comparing expression of a number of oxidative stress markers using microarray analysis have shown that TfR1 is highly expressed in the organ of Corti, modiolus and stria vascularis of the inner ear of P3-5 rats (Mazurek et al. 2011). In contrast to these latter results, our studies suggest that TfR1 is essentially undetectable in the organ of Corti in P3 rats; however, in the adult, TfR1 was observed in both the nucleus and cell surface of hair cells and also in the inner pillar cells. TfR1, was, however present in the SGN and in the cytoplasm of MC of stria vascularis of P3 rats. Prior studies have indicated that expression of TfR1 in brain capillary endothelial cells remained constant regardless of age, although, consistent with our findings, expression of neuronal TfR1 was almost absent at late embryonic and early postnatal age (Moos et al. 1998). In the adult cochlea, TfR1 staining was also observed in SGN and MC as well as blood vessels in the intermediate cell region of stria vascularis and the nucleus of the epithelium of the stria vascularis. Why TfR1 was localized in the nucleus is not known but this observation is unlikely to be an artifact of the staining procedure as its presence in the nucleus is cell specific. In addition, nuclear localization of TfR1 has previously been reported in brain tissue (Malik et al. 2011). It is also noteworthy that TfR1 labeling overlapped with at least one of the forms of DMT1 in all areas of the inner ear which is consistent with its role in the uptake of iron via DMT1.

One of the most significant findings in this paper is the presence of both Zip8 and Zip14 in hair cells. As noted above, prior studies from our laboratory (Ding et al. 2011b) using organotypic cultures demonstrated that Mn was toxic to hair cells even though they do not contain DMT1 suggesting that other transport systems are needed for the uptake of Mn. Our results demonstrating that both Zip8 and Zip14 are on the face of cuticular plate of hair cells suggest that these transporters may be the main site for entrance of Mn into these cells and thus, may be responsible for Mn toxicity. Interesting, although DMT1 was absent in the outer hair cells, results reported in this paper reveal that TfR1 which interacts with this transporter was present in these cells.

The present results add to our previous studies describing the location of the major transport proteins responsible for the uptake of Fe and other divalent metals in the inner ear. Similar to what was found for DMT1, our findings are the first to demonstrate that the distributions of both Zip8 and Zip14 are altered during development presumably to meet the changing needs of the cells to maintain normal levels of iron and other essential metals. Because the pH of the interstitial fluid within the inner ear is close to neutrality, participation of the two Zip transporters in the accumulation of these metals may be significant.

Acknowledgments This research was supported by a Grant from the National Institute for Occupational Safety and Health, R01 OH010235. We thank Dr. D. Kosman for supplying Zip8, Zip14 and TfR1 antibodies used in these studies.

Conflict of interest There is no conflict of interest that affect objectivity in regard to publishing this paper.

References

Basinger MA, Jones MM, Craft WD, Walker EM Jr, Sanders MM (1987) Chelating-agent suppression of cadmium-induced hepatotoxicity. J Toxicol Environ Health 22:261–271

Bertin G, Averbeck D (2006) Cadmium: cellular effects, modifications of biomolecules, modulation of DNA repair and genotoxic consequences (a review). Biochimie 88:1549–1559

Chesler M (2003) Regulation and modulation of pH in the brain. Physiol Rev 83:1183–1221

De Silva DA, Yamao M (2007) Effects of the tsunami on fisheries and coastal livelihood: a case study of tsunami-ravaged southern Sri Lanka. Disasters 31:386–404

Ding D, He J, Allman BL, Yu D, Jiang H, Seigel GM, Salvi RJ (2011a) Cisplatin ototoxicity in rat cochlear organotypic cultures. Hear Res 282:196–203

Ding D, Roth J, Salvi R (2011b) Manganese is toxic to spiral ganglion neurons and hair cells in vitro. Neurotoxicology 32:233–241

Ding D, Allman BL, Salvi R (2012) Review: ototoxic characteristics of platinum antitumor drugs. Anat Rec 295: 1851–1867

Ding D, Salvi R, Roth JA (2014) Cellular localization and developmental changes of the different isoforms of

divalent metal transporter 1 (DMT1) in the inner ear of rats. Biometals 27:125–134

Fleming MD, Romano MA, Su MA, Garrick LM, Garrick MD, Andrews NC (1998) Nramp2 is mutated in the anemic Belgrade (b) rat: evidence of a role for Nramp2 in endosomal iron transport. Proc Natl Acad Sci USA 95: 1148–1153

Fujishiro H, Doi M, Enomoto S, Himeno S (2011) High sensitivity of RBL-2H3 cells to cadmium and manganese: an implication of the role of ZIP8. Metallomics 3:710–718

Gao J, Zhao N, Knutson MD, Enns CA (2008) The hereditary hemochromatosis protein, HFE, inhibits iron uptake via down-regulation of Zip14 in HepG2 cells. J Biol Chem 283:21462–21468

Garrick MD (2011) Human iron transporters. Genes Nutr 6:45–54

Garrick MD, Singleton ST, Vargas F, Kuo HC, Zhao L, Knopfel M, Davidson T, Costa M, Paradkar P, Roth JA, Garrick LM (2006) DMTI: which metals does it transport? Biol Res 39:79–85

Girijashanker K, He L, Soleimani M, Reed JM, Li H, Liu Z, Wang B, Dalton TP, Nebert DW (2008) Slc39a14 gene encodes ZIP14, a metal/bicarbonate symporter: similarities to the ZIP8 transporter. Mol Pharmacol 73:1413–1423

Gunshin H, Mackenzie B, Berger UV, Gunshin Y, Romero MF, Boron WF, Nussberger S, Gollan JL, Hediger MA (1997) Cloning and characterization of a mammalian proton-coupled metal-ion transporter. Nature 388:482–488

Gunter TE, Gerstner B, Gunter KK, Malecki J, Gelein R, Valentine WM, Aschner M, Yule DI (2013) Manganese transport via the transferrin mechanism. Neurotoxicology 34:118–127

He L, Girijashanker K, Dalton TP, Reed J, Li H, Soleimani M, Nebert DW (2006) ZIP8, member of the solute-carrier-39 (SLC39) metal-transporter family: characterization of transporter properties. Mol Pharmacol 70:171–180

Herber RF (1992) The World Health Organization study on health effects of exposure to cadmium: morbidity studies. IARC Sci Publ 118:347–358

Huang CC, Lu CS, Chu NS, Hochberg F, Lilienfeld D, Olanow W, Calne DB (1993) Progress after chronic manganese exposure. Neurology 43:1479–1483

Hubert N, Hentze MW (2002) Previously uncharacterized isoforms of divalent metal transporter (DMT)-1: implications for regulation and cellular function. Proc Natl Acad Sci USA 99:12345–12350

Huff J, Lunn RM, Waalkes MP, Tomatis L, Infante PF (2007) Cadmium-induced cancers in animals and in humans. Int J Occup Environ Health 13:202–212

Josephs KA, Ahlskog JE, Klos KJ, Kumar N, Fealey RD, Trenerry MR, Cowl CT (2005) Neurologic manifestations in welders with pallidal MRI T1 hyperintensity. Neurology 64:2033–2039

Khalkova Z, Kostadinova G (1986) Auditory-vestibular changes in workers in ferrous metallurgy manufacture. Probl Khig 11:134–138

Korczynski RE (2000) Occupational health concerns in the welding industry. Appl Occup Environ Hyg 15:936–945

Krieger D, Krieger S, Jansen O, Gass P, Theilmann L, Lichtnecker H (1995) Manganese and chronic hepatic encephalopathy. Lancet 346:270–274

Liu X, Zheng G, Wu Y, Shen X, Jing J, Yu T, Song H, Chen J, Luo W (2013) Lead exposure results in hearing loss and disruption of the cochlear blood-labyrinth barrier and the protective role of iron supplement. Neurotoxicology 39:173–181

Liu H, Ding D, Sun H, Jiang H, Wu X, Roth JA, Salvi R (2014) Cadmium-induced ototoxicity in rat cochlear organotypic cultures. Neurotox Res 26:179–189

Liuzzi JP, Aydemir F, Nam H, Knutson MD, Cousins RJ (2006) Zip14 (Slc39a14) mediates non-transferrin-bound iron uptake into cells. Proc Natl Acad Sci USA 103: 13612–13617

Ma C, Schneider SN, Miller M, Nebert DW, Lind C, Roda SM, Afton SE, Caruso JA, Genter MB (2008) Manganese accumulation in the mouse ear following systemic exposure. J Biochem Mol Toxicol 22:305–310

Malik IA, Naz N, Sheikh N, Khan S, Moriconi F, Blaschke M, Ramadori G (2011) Comparison of changes in gene expression of transferrin receptor-1 and other iron-regulatory proteins in rat liver and brain during acute-phase response. Cell Tissue Res 344:299–312

Mazurek B, Amarjargal N, Haupt H, Fuchs J, Olze H, Machulik A, Gross J (2011) Expression of genes implicated in oxidative stress in the cochlea of newborn rats. Hear Res 277:54–60

Moos T (1996) Immunohistochemical localization of intraneuronal transferrin receptor immunoreactivity in the adult mouse central nervous system. J Comp Neurol 375: 675–692

Moos T, Oates PS, Morgan EH (1998) Expression of the neuronal transferrin receptor is age dependent and susceptible to iron deficiency. J Comp Neurol 398:420–430

Olanow CW, Good PF, Shinotoh H, Hewitt KA, Vingerhoets F, Snow BJ, Beal MF, Calne DB, Perl DP (1996) Manganese intoxication in the rhesus monkey: a clinical, imaging, pathologic, and biochemical study. Neurology 46:492–498

Pal PK, Samii A, Calne DB (1999) Manganese neurotoxicity: a review of clinical features, imaging and pathology. Neurotoxicology 20:227–238

Park RM, Bowler RM, Eggerth DE, Diamond E, Spencer KJ, Smith D, Gwiazda R (2006) Issues in neurological risk assessment for occupational exposures: the Bay Bridge welders. Neurotoxicology 27:373–384

Pelclova D, Sklensky M, Janicek P, Lach K (2012) Severe cobalt intoxication following hip replacement revision: clinical features and outcome. Clin Toxicol 50:262–265

Pinilla-Tenas JJ, Sparkman BK, Shawki A, Illing AC, Mitchell CJ, Zhao N, Liuzzi JP, Cousins RJ, Knutson MD, Mackenzie B (2011) Zip14 is a complex broad-scope metal-ion transporter whose functional properties support roles in the cellular uptake of zinc and nontransferrin-bound iron. Am J Physiol Cell Physiol 301:C862–C871

Pomier-Layrargues G, Spahr L, Butterworth RF (1995) Increased manganese concentrations in pallidum of cirrhotic patients. Lancet 345:735

Roth JA, Garrick MD (2003) Iron interactions and other biological reactions mediating the physiological and toxic actions of manganese. Biochem Pharmacol 66:1–13

Roth JA, Horbinski C, Feng L, Dolan KG, Higgins D, Garrick MD (2000) Differential localization of divalent metal transporter 1 with and without iron response element in rat

PC12 and sympathetic neuronal cells. J Neurosci 20:7595–7601

Wang CY, Jenkitkasemwong S, Duarte S, Sparkman BK, Shawki A, Mackenzie B, Knutson MD (2012) ZIP8 is an iron and zinc transporter whose cell-surface expression is up-regulated by cellular iron loading. J Biol Chem 287:34032–34043

Yang WM, Jung KJ, Lee MO, Lee YS, Lee YH, Nakagawa S, Niwa M, Cho SS, Kim DW (2011) Transient expression of iron transport proteins in the capillary of the developing rat brain. Cell Mol Neurobiol 31:93–99